Journal of Optoelectronics and Advanced Materials Vol. 3, No. 2, June 2001, p. 443 - 454

SPECTROSCOPIC STUDIES OF BULK As_2S_3 GLASSES AND AMORPHOUS FILMS DOPED WITH Dy, Sm AND Mn

M. S. Iovu, S. D. Shutov, A. M. Andriesh, E. I. Kamitsos[a], C. P. E. Varsamis[a], D. Furniss[b], A. B. Seddon[b], M. Popescu[c]

Center of Optoelectronics, Str. Academiei 1, MD-2028 Chisinau, Moldova
[a]Theoretical and Physical Chemistry Institute, HNRF, 11635 Athens, Greece
[b]Novel Photonic Glasses Group, University of Nottingham, Nottingham N67 2RD, UK
[c]National Institute for Physics of Materials, Bucharest-Magurele, Romania

The effect of rare earth (Dy and Sm) and transition metal (Mn) luminescent impurities on the optical properties of As_2S_3 glass is studied in a wide spectral region. The Raman, infrared, band-to-band and edge absorption spectroscopies are employed to obtain information about the incorporation of impurity ions in the host glass structure and the corresponding changes in intrinsic optical characteristics. The effects of light-soaking and thermal treatment on the doped As_2S_3 glasses were examined as well. In the fundamental absorption region a reflectivity maximum at 2.98 eV shows blue (Dy, Sm) or red (Mn) shift depending on the electronegativity of the impurity, in accordance with the corresponding variations of the glass structure. Near the edge absorption the impurity affects strongly the slope and the magnitude of the weak absorption tail. In the wide range of transparency the addition of impurity suppresses several absorption bands indicating the interaction of dopants with the host glass contaminations. Some variations of the characteristic Raman spectra under light exposure and thermal ageing of doped glasses were registered. The observed effects of metal dopants on the As_2S_3 glass are discussed in connection with the expected behaviour of the impurities in the glass.

(Received June 2, 2001; accepted June 11, 2001)

Keywords: As_2S_3 glass, Amorphous film, Spectroscopic study

1. Introduction

Glassy As_2S_3 is a promising candidate for optoelectronics applications because of its high transmission in the infrared (up to 10 μm), high refractive index (n≈2.4) and low phonon energy [1,2]. Special interest for applications is connected with glassy As_2S_3 doped with optically active rare-earth and transition metal ions, because they alter optical, photoelectrical and transport properties of the host material [3-5]. The bandgap of arsenic sulphide lies in the visible region of the spectrum (E_g≈ 2.4 eV), and thus optical transitions involving conduction bands and edge tail states overlap with some electronic transitions due to the discrete levels of the rare-earth ions (Pr^{3+}, Nd^{3+}, Sm^{3+} or Dy^{3+}). For this reason, the photon energy absorbed in the broad band region in rare earth doped As_2S_3 glasses is partially transferred to rare earth ions, and this results in the enhancement of the pumping efficiency of luminescence. This is an important effect for applications such as in fibre optics amplifiers operating at the 1.3 μm telecommunication window [6,7].

X-ray diffraction results as well as optical, electrical and photoelectrical characteristics have been reported for As_2S_3 and As_2Se_3 glasses doped with Dy, Sm and Mn [8]. It was shown that doping affects the interlayer distance and leads to creation of additional localised states in the forbidden gap of the chalcogenide glass. These effects are manifested by changes in electrical and photoelectrical characteristics of glass, while doping stabilises the glassy matrix with respect to light exposure and thermal treatment [9].

The aim of this paper is to study further the effect of metal impurities (Dy, Sm and Mn) on the structure of As_2S_3 glass and the optical properties measured over a wide spectral region. The influence of metal impurities on the medium range order (MRO) structure of glass was studied by X-ray diffraction, while infrared and Raman spectroscopies were applied to reveal changes in the short range order (SRO) structure. The effect of doping on the optical characteristics of As_2S_3 glass was

investigated by UV-visible spectroscopy. Combination of these experimental techniques may elucidate the way metal ions are incorporated in the glassy network, and could help to optimise chalcogenide glass compositions with the desired optical properties. Finally, the effect of illumination and annealing of arsenic sulphide bulk glasses and thin films doped with Dy, Sm and Mn was investigated by infrared and Raman spectroscopies.

2. Experimental

Chalcogenide glasses As_2S_3:Me (Me:Dy, Sm and Mn) were synthesised using elements of 6N (As, S) and 5N purity (Dy, Sm, Mn). Conventional melting in evacuated ($p \sim 10^{-5}$ Torr) and sealed silica ampoules was carried out at two temperature steps, 600÷650 °C for 2 h and 800÷850 °C for 8 h, and was followed by quenching in cold water. The nominal concentration of glass in metal ion dopants was 0.1 and 0.5 at. % (Table 1). The colour of the obtained glasses varies from yellow-red for pure As_2S_3, to dark-red for As_2S_3 doped with Dy and Sm, and to black for As_2S_3 doped with Mn. The glass transition temperature, T_g, of As_2S_3:Me glasses was measured by differential thermal analysis (DTA) and was found to be $T_g \approx 200$ °C (Table 1), as compared to $T_g = 151$ °C for the pure As_2S_3 glass [8].

As_2S_3:Me glass samples doped with various amounts of metal ions were investigated by X-ray diffraction on a Siemens Kristalloflex IV diffractometer, which was equipped with copper target tube, a graphite monochromator and a NaI(Tl) water cooled scintillation counter. It is noted that very accurate recording of the diffraction patterns was necessary because of the nature of the glass diffractograms (i.e. existence of a few broad maxima), and the expected weak structural modifications due to the low level doping with metal ions. The samples were prepared as powders, by crushing chunks of the chalcogenide glasses, and were pressed in special supports for X-ray measurements. High precision diffraction curves were obtained using the step by step method in recording the X-ray intensity. The number of X-ray quanta was counted for 20 s at every angular position, using an angular increment (2θ) from 0.0050 to 0.020.

The bulk glasses were cut into plates of 2÷3 mm in thickness using a low speed diamond saw, and then polished to yield samples with high quality flat surfaces suitable for optical measurements. As_2S_3:Me thin films of thickness 2.0 to 8.85 μm were prepared by thermal evaporation in vacuum onto K-8 glass substrates. A SolarBox-1500 device equipped with a Xenon lamp and infrared and ultraviolet cutting filters was used as light source for exposing bulk and thin film samples to radiation in the spectral region 0.7 to 0.4 μm, where As_2S_3 glass exhibits its optical bandgap (2.4 eV). Annealing bulk As_2S_3:Me glasses was accomplished by heating in an open air furnace in a step-by-step mode at 160 °C, 190 °C and 210 °C for 3 h, 2 h and 1 h, respectively. The as-deposited and irradiated As_2S_3 thin film samples were annealed at 160 °C for 1 h.

Infrared transmittance and specular reflectance (11° off-normal) spectra were recorded on a Fourier-transform vacuum spectrometer (Bruker IFS 113V). Appropriate sources (Hg arc and globar) and detectors (DTGS with polyethylene and KBr windows) were used to cover the infrared region from 30-4000 cm^{-1}. Five Mylar beam splitters of variable thickness (3.5 to 50 μm) were used in the far infrared, 30-700 cm^{-1}, and a KBr one in the mid-infrared range, 400-4000 cm^{-1}. The entire infrared spectrum was obtained by merging the six spectral segments, each one corresponding to the optimum beam splitter throughout. All spectra were measured at room temperature with a resolution of 2 cm^{-1} and represent the average of 200 scans. The reflectance data were analysed by employing the Kramers-Kronig technique to yield the optical response functions of the glass, i.e. the complex refractive index and dielectric function. The absorption coefficient spectra were calculated from the expression $\alpha = 4\pi k\nu$, where k is the imaginary part of refractive index and ν is the frequency in cm^{-1}.

Raman spectra were measured on a Fourier-transform spectrometer (Bruker RFS100) in a back-scattering geometry and resolution of 2 cm^{-1}. The 1064.4 nm line of a Nd-Y laser was used for excitation and this leads to Raman spectra free of luminescence background. UV-visible room temperature reflectance and absorption spectra were recorded on a Perkin-Elmer spectrometer (Lamda 19) in the spectral range 0.2 to 3.2 μm.

3. X-ray diffraction patterns

The measured diffraction curves have shown that all chalcogenide compositions considered in this work are completely amorphous. The main difference between the measured diffraction curves was found in angular region comprising the first sharp diffraction peak (FSDP) as shown in Fig. 1. This finding suggests that doping influences primarily the medium range order structure of the glassy network. A shift of the FSDP from its position in pure As_2S_3 glass can be observed in the diffraction curves of doped glasses (Fig. 1), the direction of which depends on the type of doping metal. We have employed the position of the FSDP in each glass to calculated the per cent relative change of the interlayer distance between As_2S_3 layers in the glassy network, $\Delta d/d$ (%), as a function of metal ion type and content.

The obtained change of interlayer distance was found to depend linearly on the per cent ionicity of the metal-sulphur bond, suggesting a direct influence of Me-S bonding on the MRO structure of glass. The As_2S_3 disordered layers are distorted locally by insertion of metal ions that bond to sulphur atoms. Me-S interactions of high covalency give rise to strong directional bonding that makes the layers more rigid, while the stiffness of layers decreases when the Me-S bonding is mainly ionic and therefore weaker. Thus, the intralayer ordering and the interlayer packing are dependent on the type of metal ions introduced in As_2S_3 glass. Samarium and dysprosium exhibit electronegativities lower than manganese, and thus assume the role of network modifier ions with ionic Me-S bonding. This effect allows for a better packing of the disordered As_2S_3 layers, which can now assume a smaller interlayer distance with respect to pure As_2S_3 glass.

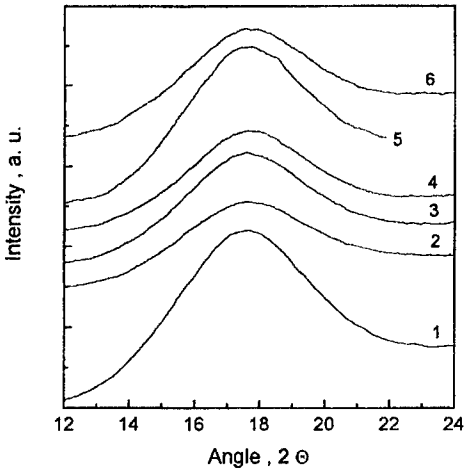

Fig. 1. X-ray diffraction curves of bulk glasses in the region of the first sharp diffraction peak (FSDP); As_2S_3 (1), As_2S_3+0.1 at.% Dy (2), As_2S_3+0.1 at.% Sm (3), As_2S_3+0.5 at.% Sm (4), As_2S_3+0.1 at.% Mn (5), and As_2S_3+0.5 at.% Mn (6).

The higher covalency of Mn-S bonding renders the Mn ions a network former role, and thus the disordered layers become stiffed by the insertion of manganese ions. This leads to an increase of the effective layer thickness and a consequent increase of the interlayer spacing. The effect of the low metal ion contents on the As_2S_3 glass can be explained by co-operative effects. Insertion of few dispersed ions in the layer structure can induce a (dis)ordering effect on a scale larger than the distance of the first co-ordination sphere and, therefore, the interference between the induced zones can amplify the (dis)ordering effect.

4. UV-VIS reflectivity spectra in the fundamental absorption region

The reflectivity spectra of the bulk glassy samples with composition As_2S_3 and As_2S_3:Me (Me:Sm, Dy, Mn) are presented in Fig. 2. The spectra of As_2S_3:Me glasses are normalised to the As_2S_3 spectrum at the photon energy of 2.6 eV, which is near the fundamental absorption edge. This

normalisation procedure removes difference in reflectivity of about 8 % due to surface imperfections of the glass samples.

In the photon energy interval between 2.5 and 6.2 eV a broad double reflectivity peak is observed in accordance with results of earlier studies [2, 10-12], and can be attributed to electronic transitions from the valence band to the conduction band minimum. According to band structure calculations in a tight-binding approximation [13,14], the states near the valence band edge of As_2S_3 result predominantly from the p-orbital electron lone-pair of the chalcogen atom (low-energy side of the reflectivity peak in Fig.2), and the high-energy side of the peak is due to p- and σ- orbital states of chalcogen. In addition to chalcogen orbitals, both parts contain contributions of the p- and s-orbitals of arsenic. In this approximation the shape of the spectra is governed by the SRO structure of glass.

Watanabe et al. [15] have pointed out the important role of intermolecular interactions in chalcogenide glasses, which are responsible for the strong dependence of the optical gap on external pressure. The inclusion of intermolecular interactions leads to marked changes in the density-of-states spectra of the valence bands, resulting in the smoothing and broadening of their characteristics. Such changes are observed in the reflectivity spectra in Fig. 2 with addition of metal impurity. Introduction of rare earth Sm and Dy ions causes the broadening of the main reflection feature, especially around its high-energy peak at 3.5 eV, as quoted in earlier studies [10].

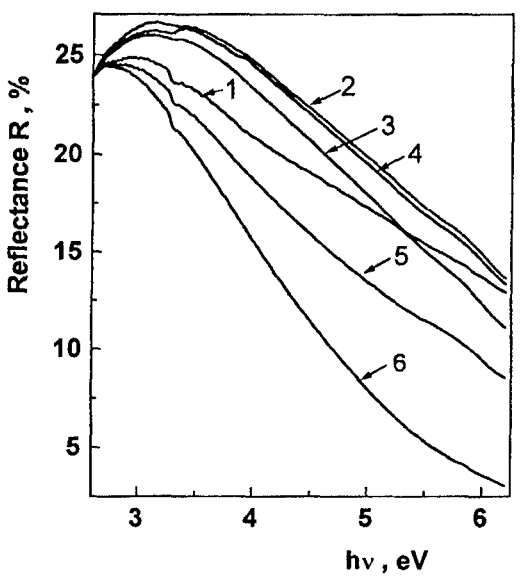

Fig. 2. Reflectance spectra of bulk glasses; As_2S_3 (1), As_2S_3+0.1 at.%Dy (2), As_2S_3+0.1 at.%Sm (3), As_2S_3+0.5 at.%Sm (4), As_2S_3+0.1 at.%Mn (5) and As_2S_3+0.5 at.%Mn (6).

However, addition of the transition metal Mn ions to As_2S_3 glass decreases the reflectivity and bandwidth of the aforementioned band. As shown in Fig. 2, the induced changes by metal ion doping increase with increasing impurity content from 0.1 to 0.5 at. % Sm and Mn. The fall of reflectivity in the 5 to 6 eV energy range in the presence of metal impurities may be associated with the effect of impurities on the degree of intermolecular interactions, which influence significantly the density of states in this energy range [15]. The changes in intermolecular interactions were found to be reflected in the increase (Mn) or decrease (Sm and Dy) of the interlayer distance as discussed earlier in this work. However, these observations are insufficient to provide a quantitative explanation of the impurity effect on the presented reflectivity spectra since the magnitude of shifts predicted in [15] is not observed here. This may suggest that the effect of metal ion impurities is considerably more complex.

5. Fundamental edge absorption

In chalcogenide glasses the absorption edge is broader than in crystalline analogues and this is caused by a broad energy distribution of electronic states in the band gap due to disorder and defects. The absorption edge in the high absorption region ($\alpha > 10^4$ cm^{-1}) is described by a quadratic function

$$\alpha \propto \frac{1}{h\nu}(h\nu - E_g)^2, \quad (1)$$

and when plotted in the Tauc co-ordinates $(\alpha \cdot h\nu)^{1/2}$ vs. $(h\nu)$ [16] gives the value of the optical gap, E_g, determined as the energy difference between the onsets of exponential tails of the allowed conduction bands [17]. For amorphous As_2S_3 the value of band gap was found to be $E_g = 2.35 \div 2.4$ eV [2].

The optical absorption edge spectra of As_2S_3 doped thin films are presented in Fig. 3a. As in the case of bulk glasses, doping the evaporated As_2S_3 thin films affects strongly the optical absorption edge spectra, as evidenced by the pronounced shift to lower energy values.

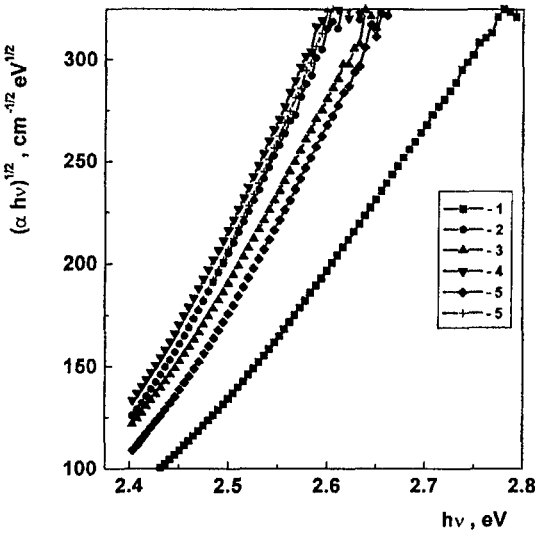

Fig.3a. Absorption spectra of thin films; As_2S_3 (1), As_2S_3+0.1 at.% Dy (2), As_2S_3+0.1 at.% Sm (3), As_2S_3+0.5 at.% Sm (4), As_2S_3+0.1 at.% Mn (5) and As_2S_3+0.5 at.% Mn (6).

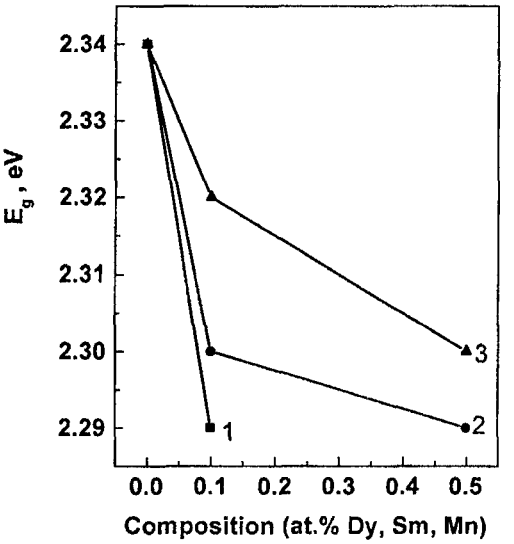

Fig. 3b. Dependence of the optical band gap, E_g, for As_2S_3 doped thin films on the type and content of metal ion impurity; Dy (1), Sm (2) and Mn (3).

The optical gap E_g determined by extrapolation of the straight-line portions of the $(\alpha \cdot h\nu)^{1/2}$ vs. $(h\nu)$ graphs was found to be 2.34 eV for As_2S_3 (Fig. 3b and Table 1), in good agreement with previously reported data [2]. Doping As_2S_3 glass with metal impurities was found to decrease E_g (Table 1), with the new optical gap value being dependent on the nature and concentration of the metal ion dopant (Fig. 3b).

Table 1. Glass transition temperature, T_g, optical band gap, E_g, and Δ_1, Δ_2 values of As_2S_3 doped glasses.

Glass Composition	T_g, °C	E_g, eV	Δ_1, eV	Δ_2, eV
As_2S_3	151	2.34	0.056	0.31
As_2S_3+0.1 at.% Dy	205	2.29	0.11	0.31
As_2S_3+0.1 at.% Sm	213	2.30	0.07	1.02
As_2S_3+0.5 at.% Sm	207	2.29	0.07	1.02
As_2S_3+0.1 at.% Mn	196	2.32	-	0.31
As_2S_3+0.5 at.% Mn	197	2.30	-	-

Absorption coefficient spectra, α, of bulk glasses were calculated from transmittance, T, and reflectance, R, measurements according to:

$$\alpha = \frac{-\ln T}{d} + \frac{2\ln(1-R)}{d}, \tag{2}$$

where d is the thickness of the sample, and are shown in Fig.4. In the Urbach edge region ($\alpha \approx 1 \div 10^3$ cm^{-1}) the absorption coefficient spectra depend exponentially on the photon energy

$$\alpha \propto \exp(\frac{h\nu}{\Delta_1}), \tag{3}$$

where Δ_1 is the parameter which characterises the distribution of localised states in the band gap. In this region the experimentally obtained α spectrum for vitreous As_2S_3 is similar to that reported earlier [16]. In addition, the Δ_1 value for amorphous As_2S_3 found in this work, Δ_1=0.056 eV, is in good agreement with the reported value of 0.05 eV [16], whereas for As_2S_3 doped with Dy and Sm Δ_1 is found to be somewhat higher (Table 1). For As_2S_3 doped with Mn the absorption coefficient in this region is very high, and almost frequency independent for the 0.5 at. % Mn glass. The broadening of the Urbach tail is caused probably by the formation of new impurity metal-based structural units, which add compositional disorder to the existing structural disorder. The reason for such behaviour and the role of disorder in the formation of the Urbach edge is still under discussion [18]. This effect is possibly responsible for the drastic increase of absorption in samples doped with Mn, where new Mn-based structural units with lower optical threshold energy may be formed resulting in the decrease of the mean value of the gap as in the case of alloys.

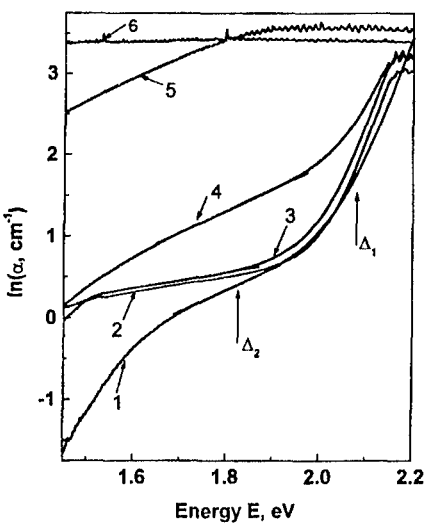

Fig. 4. The absorption spectra of bulk glasses; As_2S_3 (1), As_2S_3+0.1 at.%Sm (2), As_2S_3+0.5 at.%Sm (3), As_2S_3+0.1 at.%Dy (4), As_2S_3+0.1 at.%Mn (5) and As_2S_3+0.5 at.%Mn (6).

The absorption coefficient spectra in the region of weak absorption (α<1 cm^{-1}) are also included in Fig. 4 and show that doping with Sm and Dy results in an increase of the absorption coefficient. The effect of Mn doping is much more pronounced and leads to very high absorption coefficient values. It is known that in this region the absorption coefficient depends strongly on the conditions of sample preparation and the impurities present, and this is often described by an exponential dependence:

$$\alpha \propto \exp(\frac{h\nu}{\Delta_2}), \tag{4}$$

where $\Delta_2 > \Delta_1$ [16]. The value of Δ_2 for vitreous As_2S_3 obtained in this work is $\Delta_2 \approx 0.31$ eV, and this in good agreement with the reported value of 0.3 eV [2]. Doping As_2S_3 was found to affect drastically Δ_2 as shown by the values reported in Table 1.

The nature of the weak absorption tails in chalcogenide glasses remains to be investigated. It is demonstrated that the absorption in this region is sensitive to impurities, though the tail is still

observed in specially purified samples. This weak absorption may be attributed to additional states created by defects and/or impurities, or to the increase in the average amplitude of the internal electric fields produced by the introduction of additional charged centres. The latter interpretation can be applied to the present case since Sm/Dy and Mn dopants enter the host glass as three- and two-fold charged ions, respectively. It is noted that the As_2S_3 glass studied in this work shows absorption in the region under consideration which is about an order of magnitude higher than that of specially purified samples employed for fibre-optic applications. .

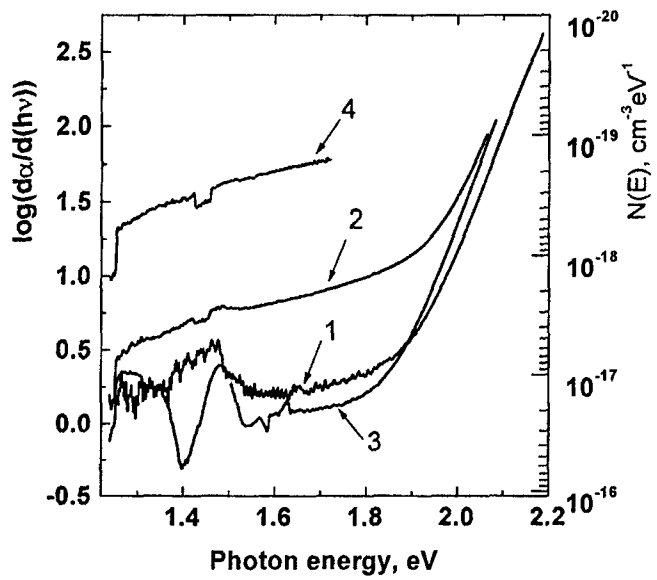

Fig. 5. Derivative of absorption spectra reported in Fig. 4. Right scale gives the order of the density of states. Spectral numbering corresponds to glass compositions given in the caption of Fig. 4.

For the evaluation of the density of states distribution associated with the weak absorption region we follow the approach of Ref. [19]. By using standard simplifying assumptions the relation between the density of states N(E) and absorption spectrum α(hν) takes the form [20]:

$$N(E_c\text{-}h\nu) = M[d\alpha/d(h\nu)], \quad (5)$$

where $M \approx 10^{17}$ cm^{-2}. The density of states N(E) calculated from the differentiation of the α(hν) spectra are shown in Fig. 5 for the As_2S_3:0.1at.% Me glass samples. It is observed that the Sm doped sample modifies slightly the density of states in the depth of the gap, while doping with Dy and especially Mn produces a substantial increase in the whole energy range. This procedure provides reasonable values for the density of states of active centres, and this is ca. 10^{17} $cm^{-3}eV^{-1}$. As shown in Fig. 5 Dy and particularly Mn ions are more effective in producing optically active centres in As_2S_3 than Sm ions.

6. MID infrared transmittance

The mid-IR transmission spectra of As_2S_3 and As_2S_3:Me doped glasses are shown in Fig. 6 and are characterized by several well resolved absorption bands. These bands are observed in the frequency ranges 839÷993 cm^{-1} (As-OH), 1500÷1587 cm^{-1} (O-H), 2487÷2493 cm^{-1} (S-H), and 3539÷3625 cm^{-1} (O-H), and are summarized in Table 2. The characteristic absorption bands for pure As_2S_3 are measured at about 993, 1587, 2487, and 3539÷3625 cm^{-1}, and are significantly reduced upon doping with Sm, Dy and Mn. For the As_2S_3+0.5at.% Sm glass additional absorption bands are measured at 2025 and 1500 cm^{-1}. The observed changes upon doping in the mid infrared region are most likely related to interactions of a portion of the introduced metal ion impurities with the inherent

impurities of the host glass, such as hydrogen and oxygen atoms. Such interactions result in the reduction of the relative intensity of bands associated with O-H. S-H, As-O and As-H bonds in the parent glass.

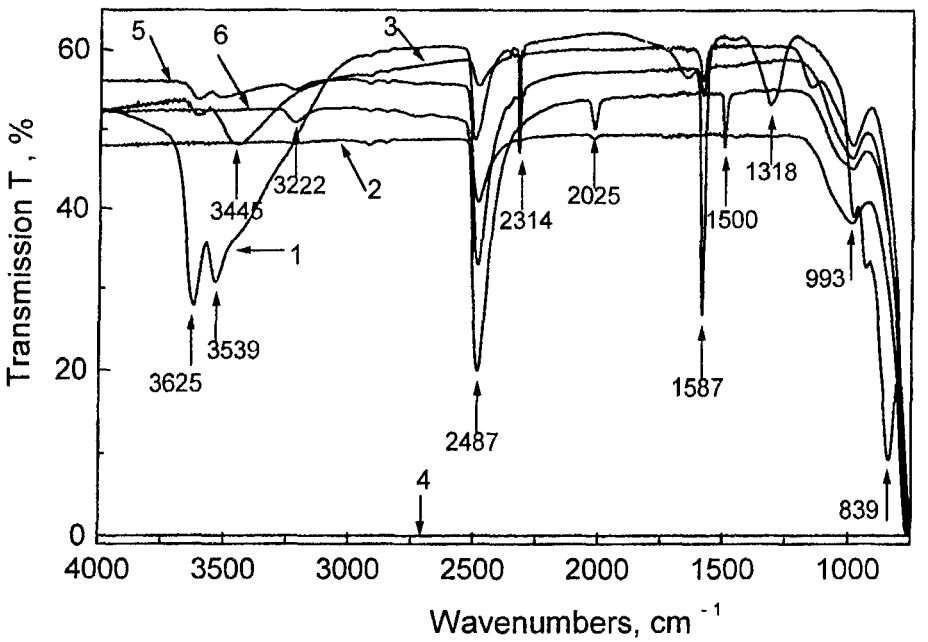

Fig. 6. Mid infrared transmission spectra of glasses As_2S_3 (1), As_2S_3+0.1 at.% Dy (2), As_2S_3+0.1 at.% Mn (3), As_2S_3+0.5 at.% Mn (4), As_2S_3+0.1 at.% Sm (5), and As_2S_3+0.5 at.% Sm (6).

Table 2. Assignments of characteristic vibrational bands for vitreous As_2S_3 doped with Dy, Sm and Mn.

Glass composition	**Infrared frequency (cm^{-1}) and assignments**					
	O-H	**S- H**	**?**	**O-H**	**As_4O_6**	**As–O As–H**
As_2S_3	3539-	2487	2314	1587	1318	839
As_2S_3+0.1 at.% Dy	3625	2493	-	-	-	993
As_2S_3+0.1 at.% Sm	-	2493	2325	1590	-	989
As_2S_3+0.5 at.% Sm	3623	2493	2024	1500	-	990
As_2S_3+0.1 at.% Mn	3623 3460	2493	-	1590	-	988

Additional treatment of glasses by irradiation for 6 hours and annealing at 210 °C was found to cause no significant changes in the infrared transmission spectra. This fact manifests the high stability of As_2S_3-based bulk glasses towards thermal and visible light-irradiation treatments. However, a recent study of bulk As_2S_3 glass has shown that wavelength-selective infrared irradiation can cause a significant reduction of the intensity of vibrational modes associated with CH_x impurities [21]. Thus, the method of wavelength-selective infrared irradiation may provide a novel non-thermal treatment for the reduction of infrared absorption attributed to impurities in As_2S_3-based glasses.

7. Raman spectra

a). Raman spectra of As_2S_3 doped glasses

The measured Raman spectra of As_2S_3 and As_2S_3:Me doped glases are reported in Fig.7. The Raman spectrum of vitreous As_2S_3 is similar to that reported in the literature [22,23], and is dominated by the strong band at ca. 345 cm^{-1} attributed to the symmetric stretching vibrational mode of $AsS_{3/2}$ pyramids [24]. Besides this strong band at 345 cm^{-1}, there are additional features (shoulders) at ca. 310 and 380 cm^{-1} and can be assigned to the asymmetric stretching modes of $AsS_{3/2}$ pyramids and As-S-As bridges, respectively [24]. The presence of sulphur in excess is indicated by the weak band at 485÷495 cm^{-1} associated with the S-S stretching vibration in S_8 rings. Weak bands situated at 188 and 235 cm^{-1} can be attributed to the bending modes of $AsS_{3/2}$ pyramids and S_8 and As_4S_4 molecules [23,24].

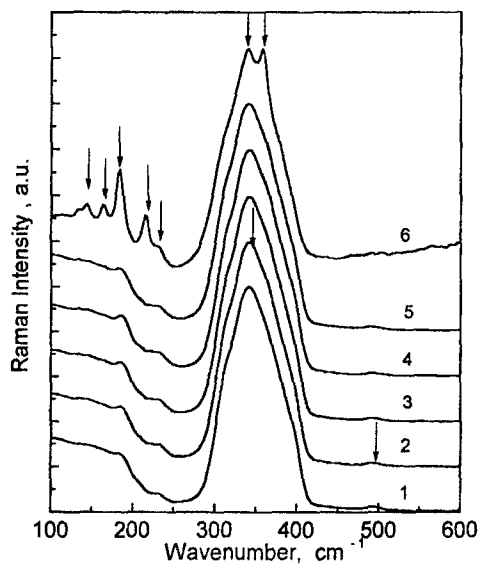

Fig. 7. Raman spectra of chalcogenide glasses; As_2S_3 (1), As_2S_3+0.1 at.% Dy (2), As_2S_3+0.1 at.% Sm (3), As_2S_3+0.5 at.% Sm (4), As_2S_3+0.1 at.% Mn (5), and As_2S_3+0.5 at.% Mn (6).

Doping As_2S_3 glass with Dy and Sm causes a slight increase of the intensity of bands located at 235 and 185 cm^{-1}, as opposed to the drastically changed Raman spectrum of the As_2S_3+0.5 at.% Mn glass. In particular, introduction of Mn leads to the appearance of a number of narrow bands in the frequency region 130 to 220 cm^{-1} which may be associated with the formation of a new sulphur-containing units, like the MnS clusters. In addition, the most intense peak at 345 cm^{-1} splits into two bands characteristic of the presence of As-rich molecular units (As_4S_4 type molecules), as reported elsewhere [23]. Such new molecular fragments can be formed by a Mn-induced dissociation $2As_2S_3 \rightarrow As_4S_4+S_2$. A similar dissociation process was suggested by the Raman spectral profiles of freshly evaporated amorphous chalcogenide films in the As-S system [23].

b). Raman spectra of light irradiated As_2S_3 doped bulk glasses

With the exception of the As_2S_3+0.5 at.% Mn glass, irradiation with light in the visible was found to cause no effect on the Raman spectra of all other compositions. Similar observations were reported in a recent study of photodarkening effects in glassy As_2S_3 [25]. Irradiation with light of energy near the optical band gap (λ=514.5 nm) for 230 hours resulted only in subtle differences in the measured NMR spectra [25]. It is pointed out that an increase of the relative intensity of the broad

band situated at 345 cm^{-1} during irradiation was observed in the Raman spectra of crystalline As_2S_3 samples and was ascribed to a crystal-to-amorphous state transition [17].

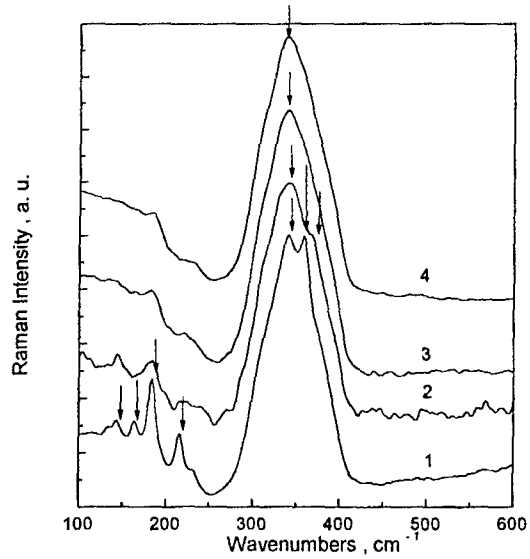

Fig. 8. Raman spectra of As_2S_3+0.5 at.%Mn glass before anealing (1) and after annealing at T=150 °C for 3 hours (2), at T=190 °C for 2 hours (3), and at T=210 °C for 1hour (4).

c). Raman spectra of annealed As_2S_3 doped glasses

The Raman spectrum of As_2S_3 glass was found to remain the same after annealing at temperatures T=150 °C (t=3 hours), T=190 °C (t=2 hours) and T=210 °C (t=1 hour). Frumar et al. [26] suggested that the As_2S_3 glass does not crystallise even after annealing for several months at temperatures near or above the glass transition temperature. These findings indicate again the high thermal stability of As_2S_3 glass, probably because of similarities in the short range order structure and Gibbs free energy in the glassy and crystalline states of arsenic sulfide.

The same behaviour was observed for the doped As_2S_3 glasses with the exception of the As_2S_3+0.5 at. % Mn glass. As shown in Fig.8, upon increasing annealing temperature the splitting of the peak at ca. 345 cm^{-1} gradually disappears, and is completely removed with annealing at 210 °C. This effect is accompanied by the progressive decrease of the intensity of the sharp bands in the 130 to 220 cm^{-1} region. Thus, the dissociation process $2As_2S_3 \rightarrow As_4S_4+S_2$ seems to be reversed by annealing. Similar effects were reported in photodarkening studies of glassy As_2S_3 where changes induced by irradiation at 514.5 nm for 230 h were found to be reversed by annealing at 200 °C for 1.75 h [25].

d). Raman spectra of light irradiated As_2S_3 thin films

The Raman spectrum of the as-evaporated As_2S_3 thin film measured in this work was found to be similar to that reported in a previous study [28]. This spectrum exhibits strong bands at 345 and 365 cm^{-1}, and several sharp features in the region 100 to 250 cm^{-1} (Fig. 9a), which can be assigned to molecular species of the As_4S_4, As_4 and S_n type.

Irradiation of As_2S_3 thin films prepared by thermal evaporation was found to cause a photodarkening effect, as manifested by measurements of the absorption edge of thin films (L=8.85 μm) before and after irradiation. It was found that irradiation causes a shift of the absorption edge in the Urbach region to lower energies. This shift is equal to $\Delta\lambda$=6.3 nm when the film is irradiated for 20 min, and increases to $\Delta\lambda$=16.8 nm when the film is irradiated for 6 hours.

As shown in Fig.9a, irradiation treatment for 20 and 40 min causes the decrease in the intensity of bands at 364 and 495 cm^{-1} and those in the frequency region 100 to 250 cm^{-1}, in agreement with results reported in previous works [27,29]. When the irradiation time was increased

to 6 hours the glass exhibited a broad Raman spectrum with a pronounced feature at 231 cm^{-1} (Fig. 9a), which may by associated with As clustering in the glass [19]. Such changes may be interpreted in terms of optical polymerization of As_4S_4 structural units into the glassy network, as reported previously in a study of photoinduced changes in the infrared spectrum of amorphous As_2S_3 films [30].

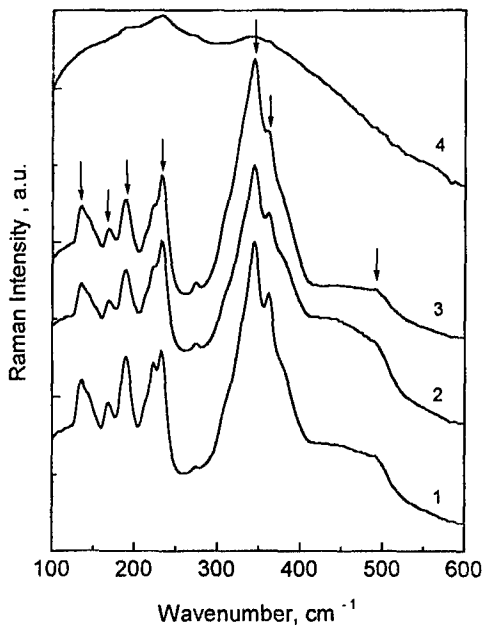

Fig. 9a. Raman spectra of the as-deposited As_2S_3 thin film (1), and after irradiation for 20 min (2), 40 min (3), and 6 h (4).

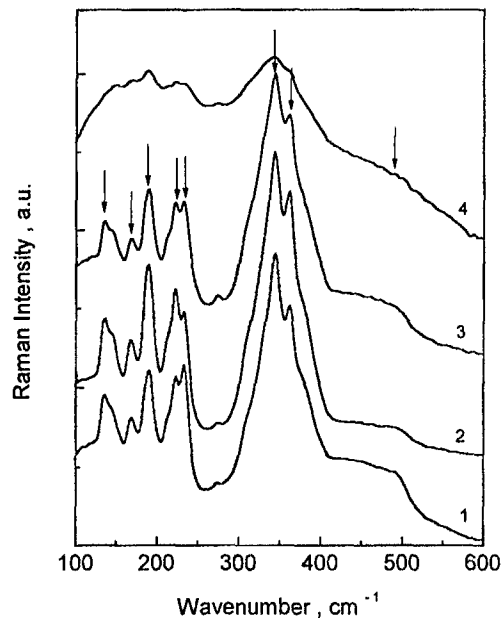

Fig. 9b. Raman spectra of as-deposited As_2S_3 thin film (1), as-deposited and annealed As_2S_3 thin film (2), after irradiation for 40 min and annealing (3) and after irradiation for 6 h and annealing at 160 °C (4).

e). *Raman spectra of annealed As_2S_3 thin films*

The effect of annealing on the as-evaporated and irradiated As_2S_3 thin films has been also investigated by Raman spectroscopy, as shown by typical spectra in Fig.9b. Annealing thin films which were irradiated for times up to 40 min causes the increase of the relative intensity of the band at 364 cm^{-1} and the decreases of the intensity of the band at ca. 495 cm^{-1}, while the features in the region 100 to 250 cm^{-1} remain relatively unaffected. The spectrum of the annealed As_2S_3 thin film which was irradiated for long time (6 hours) shows pronounced differences, and this can be understood in terms of reversing the dissociation process $2As_2S_3 \rightarrow As_4S_4+S_2$ as in the case of bulk glasses.

8. Conclusions

The effect of rare earth (Dy and Sm) and transition metal (Mn) luminescent impurities on the optical properties of the As_2S_3 glass is studied in a wide spectral region. Raman, infrared and band-to-band reflectance, and edge absorption spectroscopies are used to obtain information regarding the incorporation of impurity metal ions in the host glass structure and the corresponding changes in the intrinsic optical characteristics. The effects of light-soaking and thermal treatment on the doped As_2S_3 glasses were examined as well. In the fundamental absorption region a reflectivity maximum at 2.98 eV shows blue (Dy, Sm) or red (Mn) shift depending on the electronegativity of the impurity, in accordance with corresponding variations of the glass structure. Near the edge absorption the impurity strongly affects the slope and the magnitude of weak absorption tail. In the wide range of infrared transparency the addition of impurity suppresses several absorption bands indicating the interaction of dopants with host glass contaminations. Illumination for 6 hours in the visible and prolonged annealing at 210 °C did not affect substantially the shape and intensity of the main vibrational bands of the investigated bulk glasses, with the exception of the As_2S_3+0.5 at.% Mn composition. The

observed effects of metal dopants on the spectroscopic properties of As_2S_3 glass were discussed in connection with the chemical characteristics of the impurity metal ions.

Acknowledgment

M.S. Iovu is grateful to the Royal Society and to the NATO Scientific Committee for supporting his collaboration with the research teams at the University of Nottingham, UK, and at the National Hellenic Research Foundation (Athens-Greece), respectively. Partial support of this work was provided also by the INTAS Grant Nr. 99-1229.

References

[1] A. Madan, M. P. Shaw. The Physics and Application of Amorphous Semiconductors, Academic Press, 1988.
[2] M. Popescu, A. Andriesh, V. Chumash, M. Iovu, S. Shutov, D. Tsiuleanu, The Physics of Chalcogenide Glasses, Ed. Stiintifica Bucharest - I.E.P.Stiinta, Chisinau, 1996.
[3] S. R.Elliott, Adv. Phys. **36**, 135 (1987).
[4] A. Andriesh, M. Popescu, M. Iovu, V. Verlan, S. Shutov, M. Bulgaru, E. Colomeyco, S. Malcov, M. Leonovici, V. Mihai, M. Steflea, S. Zamfira, In: Proc. 18th Annual Semicond. Conf. CAS'95, Sinaia (Romania), Oct. 1995 (**Vol.1**, p.83).
[5] M. S. Iovu, N. N. Syrbu, S. D. Shutov, I. A. Vasiliev, S. Rebeja, E. Colomeyco, M. Popescu, F. Sava, Phys. Stat. Sol.(a), **175**, 615 (1999).
[6] S. Tanabe, J. Non-Cryst. Sol. **259**, 1 (1999).
[7] S. G. Bishop, D. A. Turnbull,B. G. Aitken, J. Non-Cryst.Sol. **266&269**, 876 (2000).
[8] M. Iovu, S. Shutov, M. Popescu, D. Furniss, L. Kukonnen, A. B. Seddon, J. Optoel. Adv. Mater. **1**, 15 (1999).
[9] M. S. Iovu, S. D. Shutov, S. Z. Rebeja, E. P. Colomeyco, M. Popescu, Phys. Stat. Sol. (a) **181**, 529 (2000).
[10] A. M. Andriesh, V. V. Sobolev, I. N. Lerman, Izv. AN MSSR, Ser.fiz.-mat.nauk, **6**, 91 (1967).
[11] R. Zallen, M. L. Slade, A. T. Ward, Phys. Rev.B **3**, 4257 (1971).
[12] N. F. Mott, E. A. Davis, Electron Processes in Non-crystalline Materials (Clarendon Press, Oxford) 1979.
[13] S. G. Bishop, N. J. Shevchik, Phys. Rev. B **12**(4), 1567 (1975).
[14] D. W.Bullet, Phys.Rev. B (1976), **14**(4), 1683
[15] J. Watanabe, H. Kawazoe, M. Yamane, J. Non-Cryst.Sol. **95&96,** 365 (1987).
[16] D. L. Wood, J. Tauc, Phys. Rev. **B5**, 3144 (1972).
[17] W. B. Jackson, S. M. Kelso, C. C. Tsai, J. W. Allen, S.-J. Oh, Phys. Rev. **B31**, 5187 (1985).
[18] J. Ihm, Solid State Commun. **53**, 293 (1985).
[19] K. Pierz, H. Mell, J. Terukov, J. Non-Cryst. Solids, **77&78**, p.1, 547 (1985).
[20] α(hv) is governed by optical transitions from the filled localised states into the free states of the conduction band; dipole matrix element of a transition is energy independent; the distribution of delocalized states is approximated by a step function.
[21] P. Hari, C. Cheney, G. Leupke, S. Singh, N. Tolk, J. S. Sanghera, I. D. Aggarwal, J. Non-Cryst. Sol. **270**, 265 (2000).
[22] G. Lucovsky, R. Martin, J. Non-Cryst. Solids **8&10,** 185 (1972).
[23] M. Frumar, Z. Polák, Z. Černošek, J. Non-Cryst. Solids **256&257**, 105-110 (1999).
[24] E. I. Kamitsos, J. A. Kapoutsis, I. P. Culeac, M. S. Iovu, J. Phys. Chem. **B101,** 11061 (1997).
[25] P. Hari, T. Su, P. C. Taylor, P. L. Kuhns, W. G. Moulton, N. S. Sullivan, J. Non-Cryst. Solids **266&269**, 929 (2000).
[26] M. Frumar, A. P. Firth, A. E. Owen, J. Non-Cryst. Sol. **192&193,** 447 (1995).
[27] I. M. Pecheritsyn, I. I. Kryzhanowsky, M. D. Mikhailov, Glass. Phys. Chem, **24**, 508 (1998).
[28] M .Frumar, A. P. Firth, A. E. Owen, Philos.Mag. **B50**, 463 (1984).
[29] A. V. Stronski, M.Vlcek, A. I. Stetsun, A. Skelenas, P. E. Shepeliavy, J. Non-Cryst. Sol **270**, 129 (2000).
[30] H. Strom, T. P. Martin, Solid State Communic. **29**, 527 (1979).